PBPK modeling of the cis- and trans-permethrin isomers and their major urinary metabolites in rats

Marie-Emilie Willemin, Sophie Desmots, Rozenn Le Grand, François Lestremau, Florence Anna Zeman, Eric Leclerc, Christian Moesch, Céline Brochot

PBPK modeling of the *cis*- and *trans*- permethrin isomers and their major urinary metabolites in rats

Marie-Emilie Willemin [a, b, 1], Sophie Desmots [c], Rozenn Le Grand [d], François Lestremau [e], Florence A. Zeman [a], Eric Leclerc [b], Christian Moesch [d], Céline Brochot [a, *]

[a] Institut National de l'Environnement Industriel et des Risques (INERIS), Unité Modèles pour l'Ecotoxicologie et la Toxicologie (METO), Parc ALATA BP2, 60550 Verneuil en Halatte, France

[b] Sorbonne University, Université de Technologie de Compiègne, CNRS, UMR 7338 Biomechanics and Bioengineering, Centre de recherche Royallieu - CS 60319 - 60203 Compiègne Cedex, France

[c] Institut National de l'Environnement Industriel et des Risques (INERIS), Unité Toxicologie Expérimentale (TOXI), Parc ALATA BP2, 60550 Verneuil en Halatte, France

[d] Centre Hospitalo-Universitaire de Limoges, Service de Pharmacologie et de Toxicologie – Pharmacovigilance, 2, avenue Martin Luther King, 87042 Limoges, France

[e] Institut National de l'Environnement Industriel et des Risques (INERIS), Unité Innovation pour la Mesure (NOVA), Parc ALATA BP2, 60550 Verneuil en Halatte, France

[1] Present address :

US Food and Drug Administration (FDA), National Center for Toxicological Research (NCTR), Division of Biochemical Toxicology, 3900 NCTR Road, Jefferson, AR 72079, United States

[*] Corresponding author: Céline Brochot

Institut National de l'Environnement Industriel et des Risques (INERIS), Unité Modèles pour l'Ecotoxicologie et la Toxicologie (METO), Parc ALATA BP2, 60550 Verneuil en Halatte, France

Tel: +33 3 44 55 68 50

Fax: +33 3 44 55 67 67

Email: celine.brochot@ineris.fr

Abstract

Permethrin, a pyrethroid insecticide, is suspected to induce neuronal and hormonal disturbances in humans. The widespread exposure of the populations has been confirmed by the detection of the urinary metabolites of permethrin in biomonitoring studies. Permethrin is a chiral molecule presenting two forms, the *cis* and the *trans* isomers. Because *in vitro* studies indicated a metabolic interaction between the *trans* and *cis* isomers of permethrin, we adapted and calibrated two PBPK models for *trans*- and *cis*-permethrin in rats. The models also describe the toxicokinetics of three urinary metabolites, *cis*- and *trans*-3-(2,2 dichlorovinyl)-2,2-dimethyl-(1-cyclopropane) carboxylic acid (*cis*- and *trans*-DCCA), 3-phenoxybenzoic acid (3-PBA) and 4'OH-phenoxybenzoic acid (4'-OH-PBA). *In vivo* experiments performed in Sprague-Dawley rats were used to calibrate the PBPK models in a Bayesian framework. The model captured well the toxicokinetics of permethrin isomers and their metabolites including the rapid absorption, the accumulation in fat and the extensive metabolism of the parent compounds, and the rapid elimination of metabolites in urine. Average hepatic clearances in rats were estimated to be 2.4 and 5.7 L/h/kg for *cis*- and *trans*-permethrin, respectively. High concentrations of the metabolite 4'-OH-PBA were measured in urine compared to *cis*- and *trans*-DCCA and 3-PBA. The confidence in the extended PBPK model was then confirmed by good predictions of published experimental data obtained using the isomers mixture. The extended PBPK model could be extrapolated to humans to predict the internal dose of exposure to permethrin from biomonitoring data in urine.

Keywords: PBPK model, *cis/trans*-permethrin, 3-phenoxybenzoic acid, *cis*- and *trans*-3-(2,2 dichlorovinyl)-2,2-dimethyl-(1-cyclopropane) carboxylic acid, Bayesian calibration, metabolites

Introduction

Pyrethroid insecticides are used in household applications, agriculture or medicine (US EPA, 2011). Their consumption increased recently, probably in response to restrictions on the use of other insecticides such as organophosphates and organochlorines. Because pyrethroids are rapidly metabolized, human exposure is usually assessed by measuring the urinary concentrations of their metabolites, including 3-phenoxybenzoic acid (3-PBA) and *cis*- and *trans*-3-(2,2 dichlorovinyl)-2,2-dimethyl-(1-cyclopropane) carboxylic acid (*cis* and *trans*-DCCA). These metabolites can either be specific to a pyrethroid (e.g., 3-(2,2-dibromovinyl)-2,2-dimethylcyclopropane-1-carboxylic acid for deltamethrin) or common to several ones (e.g., 3-PBA). The widespread exposure of humans was confirmed in biomonitoring studies, carried out in different countries such as France, Germany, USA and Japan, where the biomarkers of exposure were detected in almost all the individuals tested (Egerer *et al.*, 2004; Heudorf *et al.*, 2006; Barr *et al.*, 2010; Ueyama *et al.*, 2010; Morgan, 2012; InVS, 2013). In particular, these different studies demonstrated the large exposure of the French population to pyrethroids since the common metabolite 3-PBA was recovered at high amounts in urine with a 2 and 3-factor compared to the other countries.

Among pyrethroids, permethrin (3-phenoxybenzyl (*1RS,3RS*;*1RS,3SR*)-*cis,trans*-3-(2,2-dichlorovinyl)-2,2-dimethylcyclo-propanecarboxylate) is one of the most commonly used especially in household applications (US EPA, 2005; Stout *et al.*, 2009). Like other pyrethroids, permethrin acts on the nervous system of insects and mammals by interfering with neuronal voltage-gated sodium channels to disrupt the function of neurons (Soderlund *et al.*, 2002; Soderlund, 2012). In mammals, permethrin is suspected to induce disturbances on the neuronal and hormonal systems. Syndrome T (aggressive sparring, fine tremors) (Verschoyle and Aldridge, 1980; Wolansky and Harrill, 2008) and reproductive modifications, especially on testosterone levels (Zhang *et al.*, 2007; Zhang *et al.*, 2008; Jin *et al.*, 2012) were observed in rats after acute and chronic exposures respectively. In humans, the reported adverse effects are skin irritation, paraesthesia or headaches depending on the routes of exposure (Lequesne *et al.*, 1981; Flannigan *et al.*, 1985; He *et al.*, 1989; Gotoh *et al.*, 1998; Bradberry *et al.*, 2005). Epidemiological studies have also shown associations between modifications of the

semen quality and the presence of pyrethroids metabolites in urines (Meeker *et al.*, 2008; Young *et al.*, 2013; Imai *et al.*, 2014).

Permethrin has four stereoisomers due to the two chiral carbons on the cyclopropane rings. The *cis*- and *trans*-isomers are comprised of enantiomers 1R,S-*cis*-permethrin and 1R,S-*trans*-permethrin. Metabolic interactions between the *cis* and *trans* isomers of permethrin have been previously observed *in vitro* using hepatic microsomes (Scollon *et al.*, 2009). The intrinsic hepatic clearances of the binary mixture were found to be reduced compared to that of the individual isomers; by 39% for *trans*-permethrin in rats and a factor 2 for both isomers in humans. Such metabolic interactions could contribute to the increased time of residence of the permethrin isomers (active form) in the body potentially predisposing the organism to its associated risks. Since the ratio of the permethrin isomers in the environment is not precisely known and is not constant, it is necessary to characterize first the toxicokinetics of each isomer separately and then link them using a specific model that accounts for their metabolic interactions.

In this paper, we propose to develop and calibrate a PBPK model for *cis*- and *trans*-permethrin in a Bayesian framework using data obtained from new *in vivo* experiments in rats exposed to the individual isomers. The PBPK model developed here is an extension of the PBPK models previously published (Tornero-Velez *et al.*, 2012; Wei *et al.*, 2013). The extended PBPK model includes the kinetic of the isomer of permethrin in additional organs and integrates the toxicokinetics of the three urinary metabolites that are commonly used as biomarkers of permethrin exposure (3-PBA, *cis*- and *trans*-DCCA) and the metabolite 4'OH-phenoxybenzoic acid (4'-OH-PBA) a major metabolite of permethrin (Takaku *et al.*, 2011).

Materials and Methods

Chemicals

Cis-permethrin (3-phenoxybenzyl(1RS)-*cis*-3-(2,2-dichlorovinyl)-2,2-dimethylcyclopropane carboxylate, 99.4% purity) and *trans*-permethrin (3-phenoxybenzyl (1RS)-*trans*-3-(2,2-dichlorovinyl)-2,2-dimethylcyclopropanecarboxylate, 99% purity) were obtained from ChemService (West Chester, USA) and Dr. Ehrenstorfer (Augsburg, Germany), respectively. The internal standards *cis*-[$^{13}C_6$]permethrin (98% purity) and *trans*-[$^{13}C_2$]DCCA (98% purity) were purchased from LGC standard (Cambridge Isotope Laboratories, USA). Corn oil was acquired from Sygma-Aldrich (St Quentin Fallavier, France).

Animals

Adult male Sprague-Dawley rats were purchased from Janvier (Genet de lisle, France). They weighed 468 g ± 21 g (mean body weight (BW) ± standard deviation (SD)) and were 90-100 days old at the time of the experiments. The experimental protocol was approved by an internal ethics committee. Each rat was housed in a cage with a 12 h light/12 h dark cycle at ambient temperature (22°C ± 2°C) and relative humidity (55 ± 15%). Food (Altromin for rat and mouse, Genestril, Royaucourt, France) and tap water were provided *ad libitum*. The rats were allowed a minimum acclimation period of 4 days before experiments. Rats were not fasted before the administration of permethrin, as it was previously done for toxicokinetic studies on deltamethrin (Godin *et al.*, 2010) and permethrin (Tornero-Velez *et al.*, 2012)

Experiments

A dose of 25 mg/kg of either *cis*- or *trans*-permethrin dissolved in corn oil (2 mL/kg) was administered to rats by gavage. The same solvent (corn oil) as the one used in previous toxicokinetic studies on pyrethroids was kept to insure reliable comparisons, since the nature of the solvent can have an impact on the absorption process in case of highly lipophilic chemicals like permethrin (Soderlund *et al.*, 2002). Based on our preliminary study (Lestremau *et al.*, 2014), at the dose of 20 mg/kg of permethrin, both parents and metabolites were quantified in most of the matrices with our

analytical procedure, and no side effects were observed in rats. The dose was increased in our current study by a 0.25-fold to insure the quantification of all the compounds in all the matrices. Access to food was provided 3 h after dosing. Groups of 4 rats were sacrificed with CO_2 at 0.5, 1, 1.5, 2, 4, 6, 10, 24, 48 h and 6 days after administration. For the time points below 24 h, the rats were housed individually in a metabolic cage until euthanasia with CO_2. Because the time residence of the rats in the metabolic cage was limited to 24 h consecutively, several groups of rats were considered for the time points 48 h and 6 days. Urine and feces were then collected on 24 h intervals and were then cumulated.

Immediately after the euthanasia of the rat, blood samples were drawn from the inferior vena cava and collected in heparinized tubes. Formic acid 1% was added V/V to blood to inhibit the metabolism of permethrin due to carboxylesterases (CE) enzymes and to preserve the stability of the compounds. The median liver lobe, the perirenal fat, the muscle of the right thigh, the right kidney, the right testis and the brain were isolated and weighed. Urine and feces were collected every day in a metabolic cage until the 6^{th} day. All matrices were frozen at -80°C until analysis. No precautions were taken during the collection of the urine since no specific procedures were described for similar studies on pyrethroids metabolites in the literature (Kühn *et al.*, 1996; Leng and Gries, 2005).

Chemical analyses

The extraction and detection of analytes in organs and feces were performed by GC-MS/MS based on the analytical method developed by Lestremau *et al.* (2014). Parent compounds *cis*- and *trans*-permethrin were dosed in each matrix and the metabolites *cis*- and *trans*-DCCA in blood, liver and feces. All the organs were thawed and ground with a mortar and a pestle and then with microbeads using a Precellys homogenizer (Bertin, Montigny le Bretonneux, France). The internal standards *cis*-[$^{13}C_6$]permethrin and *trans*-[$^{13}C_2$]DCCA were added to the matrix before the microbeads step. Then, 1 g (or mL) of the matrix (except urine), containing the target analytes and their internal standards, was treated by a methanolic/hydrochloric acid solution. This step ensures the derivatization of the metabolites and the cleavage of the conjugated metabolites. The methanolic/hydrochloric acid solution has no impact on the recovery of permethrin, as pointed out by Lestremau *et al.* (2014). The

different compounds were then extracted with toluene. The extraction of permethrin in fat was performed with an acetonitrile/dichloromethane solution containing a purification step with a blend of Strata X-AW and Na_2SO_4. A column ZB-5MS (30 m × 0. 25 mm I.D., 1 µm) and a Varian gas chromatograph 3800 coupled with a Varian ion trap mass spectrometer 4000 were used. The limits of quantification were 50 µg/L for *cis*- and *trans*-permethrin, and 25 µg/L for *cis*- and *trans*-DCCA. When a compound was detected in a sample at a concentration below the limit of quantification (LOQ), the compound concentration was set to LOQ/2. This approach is quite widely used in toxico/phamacokinetic studies (Beal, 2001; Soucy *et al.*, 2006).

Both parent compounds and metabolites DCCA, 3-PBA and 4'-OH-PBA were quantified in urine by LC-MS/MS (Le Grand *et al.*, 2012). A column Atlantis T3 (150 mm × 2.1mm I.D., 5 µm) was required with Shimadzu LC-10 AD pumps coupled with a mass spectrometric AB Sciex API-5000. The LOQ for *cis*- and *trans*-DCCA, 3-PBA and 4'-OH-PBA were 8 µg/L, 12 µg/L, 10 µg/L and 500 µg/L, respectively.

The addition of concentrated hydrochloric acid during the chemical process of the samples insures the cleavage of conjugated bound to metabolites, like 4'-OH-PBA-sulfate (Gaughan *et al.*, 1977; Kühn *et al.*, 1996). The metabolites measured in this study correspond therefore to the free form and newly free form obtained after cleaving the binding conjugation (sulfate, glucuronide). No distinction was made for each metabolite between the conjugated and unconjugated form.

Model structure

The structure of the PBPK model for *cis*- and *trans*-permethrin was based on existing PBPK models developed for Type I and Type II pyrethroids, permethrin as a mixture of the two isomers and deltamethrin (Mirfazaelian *et al.*, 2006; Godin *et al.*, 2010; Tornero-Velez *et al.*, 2012). These models included the following compartments: blood and liver where metabolism occurs, intestinal tract as the route of entry of the compound and as a metabolic site, fat in which permethrin is accumulated, brain as a target tissue for neurotoxicity, and rapidly and poorly perfused tissues. In this current work, the permethrin model proposed by Tornero-Velez *et al.* (2012) was extended to include additional compartments corresponding to tissues that were analyzed in this study, *i.e.*, testes (a potential target

tissue), muscle for which permethrin is suspected to have a high partitioning affinity (a high partition coefficient of 5.59 was estimated in the former model) and kidneys as a surrogate for the rapidly perfused tissues. In concurrence with the previous models, the distribution of permethrin (and pyrethroids in general) was described to be instantaneous in several tissues and was modelled as limited by diffusion in brain, fat, muscle, testes and poorly perfused tissues. The description of the distribution of permethrin in these latter as a diffusion-limited process enables to capture the relative slow distribution of permethrin and also to obtain a better agreement between the predictions and the observed concentrations. The other compartments including intestines, kidney, liver, and rapidly perfused tissues were described as flow-limited. The absorption was modelled as described by Godin *et al.* (2010) for deltamethrin. The oral absorption was composed of two compartments (stomach and gastro-intestinal (GI) tract) with a single constant of absorption K_i located in the GI tract. Permethrin was eliminated by metabolism in three compartments (GI tract, blood and liver) and by excretion in feces in the gut lumen (no permethrin was detected in urine). The PBPK model of *cis*- or *trans*-permethrin contains in total 10 compartments (plus the stomach and GI tract lumens) and is identical in structure for both isomers.

The PBPK models for the permethrin isomers were linked to their respective sub-models describing the kinetics of the metabolites. In rats, permethrin and its oxidized forms are metabolized by CEs in blood, liver, and to a lesser extent in small intestine. Permethrin is hydrolyzed into the metabolites *cis*- and *trans*-DCCA and the (un)oxidized form of 3-phenoxybenzoic alcohol (Ross *et al.*, 2006; Crow *et al.*, 2007). This (un)oxidized carboxylic acid part, common to several pyrethroids, is then oxidized into the forms 4'OH-phenoxybenzoic acid (4'-OH-PBA) or 3-phenoxybenzoic acid (3-PBAcid), commonly labeled as 3-PBA, in the liver by cytochromes P450 (Gaughan *et al.*, 1977; Nakamura *et al.*, 2007; Takaku *et al.*, 2011; Mikata *et al.*, 2012).

To our best knowledge, the kinetics of permethrin metabolites have not yet been modeled in rats. To extend the extrapolation from rats to humans on a physiological basis for metabolites, a reduced PBPK model was developed for *cis*- and *trans*-DCCA and calibrated using measured concentrations in blood, liver, urine and feces. This model includes three compartments; blood, liver, and the rest of

the body described as a diffusion-limited compartment. The urinary excretion was modeled in blood and the fecal excretion assumed *via* bile in liver, described by a clearance (K_{uri_DCCA}) and a first-order rate (K_{fec_DCCA}), respectively. Two-compartment models for 3-PBA and 4'-OH-PBA were developed to describe their respective urinary elimination kinetics. Metabolites were eliminated from blood to urine with a first order rate constant (K_{uri_X}), where *X* denotes the respective metabolites being described. The formation of each metabolite was dependent on the whole production of metabolites in the three metabolic sites and was expressed as a fraction ($Frac_{met\_X}$) of the total clearance of *cis*- or *trans*-permethrin:

$$\frac{dA_{met\_X}}{dt} = Frac_{met\_X} \times \left(R_{liv\_PER} + R_{GI\_PER} + R_{blo\_PER}\right) \times \frac{MW_X}{MW_{PER}} \quad (1)$$

where R_{liv_PER}, R_{GI_PER} and R_{blo_PER} are the metabolic rates of permethrin in liver, GI tract, and blood, respectively. Because the amounts were expressed in mg, the amount of metabolites produced was multiplied by the ratio of the molecular weights (MW). *Cis*- and *trans*-DCCA were assumed to be formed only in the liver as hepatic metabolism is found to be the predominant mode of metabolic pathway (Crow *et al.*, 2007).

The schematic of the models are represented in Figure 1 and the equations are provided in Supplemental material.

Model parameterization

The physiological parameters are summarized in Table 1 and were either measured in the rats used in this study (volumes) or were obtained from the literature (Waites, 1991; Brown *et al.*, 1997; Schoeffner *et al.*, 1999). All the permethrin-specific parameters were estimated using the measured concentrations in the tissues and fluids except for two metabolic rates, blood and intestinal, as our experiments were not designed to estimate the metabolic rates in all three metabolic sites (liver, intestine and blood). Since experiments *in vitro* have shown the degree of metabolism in blood and intestinal tissue to be much lower than in liver (Crow *et al.*, 2007), the blood and intestinal metabolic rates were fixed to appropriate numerical values. The blood and intestinal metabolic rates were thus fixed to 0.07 L/h/kg and 0.04 L/h/kg for *cis*-permethrin and to 0.29 L/h/kg and 0.3 L/h/kg for *trans*-

permethrin, respectively. These rates were calculated based on the extrapolation to *in vivo* of the *in vitro* results obtained in whole serum (Crow *et al.*, 2007) and intestinal microsomes of rats (Nakamura *et al.*, 2007). The study conducted by Crow *et al.* (2007) was used to specifically quantify metabolism in rat blood. The metabolic rate in blood for *trans*-permethrin was obtained by scaling the intrinsic clearance rate observed in rat serum (as the ratio of *Vmax/Km*; *Vmax* of 4.2 nmol/min/mL serum and *Km* of 29.4 μM) to the volume of serum in blood (approximately 45%) and to the blood volume in adult rats (74 mL/kg of BW) (Brown *et al.*, 1997). The intrinsic clearance of *cis*-permethrin in blood was obtained by reducing the intrinsic clearance of the *trans* isomer by 4.3 fold, corresponding to the observed ratio of the specific activity of the two isomers in rat serum in the study by Crow *et al.* (2007). The *in vivo* intestinal intrinsic clearance of *trans*-permethrin was obtained by extrapolating the slope of the formation curve of the metabolite 3-phenoxybenzoic alcohol after 10 min of exposure (Nakamura *et al.*, 2007). The physiological parameters, 2.2 mg of protein/g of intestines (Martignoni *et al.*, 2006) and 2.7 g/kg of BW for the weight of the intestines (Brown *et al.*, 1997), were used as scaling factors. A ratio of 8.6 was applied to derive the intestinal intrinsic clearance of *cis*-permethrin as observed by Nakamura *et al.* (2007) between the rates of formation of 3-phenoxybenzoic alcohol from the two isomers.

The other parameters specific to permethrin and its metabolites were estimated simultaneously in a Bayesian framework. In such analysis, each parameter is considered as a random variable and a prior probability distribution reflecting the prior knowledge on the parameter's values is assigned to each parameter. The Bayes theorem was used to update the prior distribution using the experimental data obtained in our current study (specifically, the measured concentrations of each chemicals in various tissues and fluids) in order to derive a posterior distribution that can then be viewed as a combination of the prior knowledge and the information contained in the experimental data (Gelman *et al.*, 1996; Davis *et al.*, 2012). The prior distributions assigned to the parameters to be estimated are summarized in Table 2 and Table 3. All parameters were assumed to follow a truncated normal distribution. *In vitro* experiments on metabolism and the previously published toxicokinetic models were used as prior information in our analysis. The means of the prior distributions for the partition coefficients, the

rate constants and the permeability coefficients were defined according to the values reported in previous PBPK models for permethrin and deltamethrin (Mirfazaelian *et al.*, 2006; Tornero-Velez *et al.*, 2012). The coefficients of variation were fixed to be 50% for partition coefficients and rate constants, and to be 100% for the permeability coefficients because of higher uncertainty. The means of the prior distributions for the intrinsic clearance in liver were set to 3.47 L/h/kg BW and 9.86 L/h/kg BW for *cis*- and *trans*-permethrin, respectively. These values were obtained by extrapolating *in vitro* clearances observed in human hepatic microsomes (Scollon *et al.*, 2009). The ratio of *Vmax/Km* was scaled to the *in vivo* hepatic intrinsic clearance by using the following physiological parameters, *i.e.*, 45 mg of microsomal protein/g of liver (Houston, 1994) and 34 g of liver/kg of BW (Brown *et al.*, 1997).

Some of the parameters were kept fixed as they cannot be estimated from the measured concentrations in the tissues and fluids sampled in this study. The partition coefficients of both isomers of permethrin in GI tract (PC_{gi}) and in rapidly perfused tissues (PC_{rp}) were set to the estimated value of the partition coefficient in kidney (PC_{kid}). Only for *trans*-permethrin, the partition coefficient in liver (PC_{liv}) was assumed to be equal to PC_{kid} and the one in testes (PC_{tes}) equal to the one in brain (PC_{bra}) since the compounds were not detected in these organs. The permeability coefficient of testes (PA_{tes}) for *trans*-permethrin was assumed to be three times lower than the one estimated in brain (PA_{bra}) based on the ratio of the permeability coefficients estimated for *cis*-permethrin in these organs.

For metabolites, uniform distributions were assigned to the fractions of metabolites formed from the total intrinsic clearance of each isomer of permethrin. The prior distributions of the partition and permeability coefficients and the fecal elimination rates of DCCA were similar to those of permethrin. The mean value of the urine excretion rate of the metabolites was set to be the inverse of 16.5 h, corresponding to the mean half-life of the urinary elimination of the metabolites after an ingestion of cypermethrin (Woollen *et al.*, 1992).

The likelihood on the data was assumed to follow a lognormal distribution with 15% of error for all concentrations except in blood for which 5% of error was needed to reproduce adequately the observed kinetics. The calibration of the PBPK model was performed using the average of the

concentrations obtained from the group of 4 rats euthanized at a specific time point. Markov Chain Monte Carlo methods were used to estimate the posterior probability distributions using MCSim software (Bois and Mazle, 1997). Three independent Markov chains of 10,000 iterations were run and one in two of the last 5,000 iterations were recorded. A stable posterior distribution was assumed to be reached when the convergence criterion $\hat{R}$ was below 1.1.

Evaluation of the confidence in the predictions performed by the extended PBPK model

Available data on permethrin in the literature (Tornero-Velez *et al.*, 2012) were used to assess the ability of the set of estimated values of parameters to predict concentrations in other experimental conditions. In their study, Tornero-Velez *et al.* (2012) performed *in vivo* experiments in rats for a mixture (40:60) of *cis*- and *trans*-permethrin at two oral doses, 1 mg/kg and 10 mg/kg of total permethrin, and measured the concentrations of permethrin isomers in blood and three tissues (liver, fat and brain). The extended PBPK model was run with these doses as input and their predictions were compared to the measured concentrations. Due to the observed differences in the absorption phase between the two experimental studies, two assumptions were tested using our model: 1) the PBPK model calibrated in the current study was used as is to predict the literature data; 2) the absorption parameters (K_{si} and K_{int}) were set to the values used by previous PBPK model of pyrethroids (Mirfazaelian *et al.*, 2006; Tornero-Velez *et al.*, 2012) and all the other parameters were set to the estimates obtained in our study.

Results

Observed toxicokinetics of cis- *and* trans-*permethrin and metabolites*

Both *cis*- and *trans*-permethrin were detected in blood, feces and all tissues (liver, muscle, kidneys, testes, brain and fat) at all time points. The kinetic profiles of the parent compounds in blood and in tissues are presented in Figures 2. However the levels of *trans*-permethrin were below the LOQ in liver and testes, and only the samples collected at a single time point of 1 hour in the kidneys were above this limit. The toxicokinetic profiles of the *cis* and *trans* isomers were very similar and the levels of *cis*-permethrin in all organs were always higher than that of *trans*-permethrin. The kinetic profiles of the isomers observed in blood, liver and kidneys were similar: a rapid distribution in the tissues with the observed times at maximal concentration between 1 h and 2 h and a fast elimination of the compounds in blood with a half-life of about 4.2 h for *trans*-permethrin and that of 1.5 h in the first phase of elimination of the *cis* isomer (Table 4). A second phase of elimination for *cis*-permethrin was observed in the blood and liver, with a half-life ($T_{1/2}\ \beta$) of 3.3 h and 11.7 h, respectively, suggesting a slower elimination of this isomer. Due to the relatively low number of detectable data points in liver (2) in the second phase of elimination, the estimated half-life $T_{1/2}\ \beta$ is affected by uncertainties and should be considered accordingly. As reported in previous studies, a slow diffusion of permethrin was observed in tissues such as fat, muscle and organs that have a physiological barrier like brain and testes. The values of the AUC computed using observed concentrations (AUC_{obs}) are summarized in Table 5 and confirm the kinetic profiles, also reflected in the values of half-life. The 65-fold higher AUC_{obs} in the fat tissue in comparison to that in blood emphasized the degree of accumulation of the *trans* isomer in this tissue. Similarly, the ratio of AUC_{obs} in organs to blood for *cis*-permethrin is greater than one, ranging from 1.7 in muscle to 304 in fat.

The toxicokinetics of permethrin metabolites are presented in Figure 3 and Figure 4. The concentrations of metabolites from the *trans*-isomer are consistently much higher than the ones of the *cis*-permethrin, which are in the good agreement with the observed kinetic of the parent isomers. The formation of the metabolites is rapid with the quantification of *cis*-DCCA and *trans*-DCCA in blood

and liver as early as 30 mins after the administration of the permethrin isomers. The concentrations in DCCA reach a peak at 5 h in the liver (Figure 3).

A delay of 2.5 h is observed in the times to reach maximal concentration between the parent compounds and its metabolites. The elimination of DCCA from blood and liver tissue, especially that of *trans*-DCCA, is slower compared to the rate of elimination of permethrin. The elimination of *trans*-DCCA is biphasic in nature in both the blood and liver tissue, with half-lives of 12.0 h and 30.1 h for each subsequent phase in the blood (Table 4). An accumulation of both isomers of DCCA is observed in liver, as confirmed by the high value of AUC_{obs} computed to be 245.8 µg.h/mL for *trans*-DCCA. The excretion of metabolites in urine is rapid, with a completed excretion after 24 h and a high recovery of 4'OH-PBA compared to the two other metabolites.

The linearity of the dose in permethrin was evaluated by comparing the measured concentrations in isomers of permethrin to the ones previously published in blood, liver, brain and fat of rats exposed to a mixture of isomers *cis/trans* (40:60) at 1 and 10 mg/kg. For both isomers, the normalized concentrations at the doses of 1, 10 and 25 mg/kg present similar profiles for the uptake and the elimination of permethrin. The three datasets supported the linearity of the dose for the tested organs/fluids for *cis*-permethrin. For *trans*-permethrin, we observed a slower elimination at the dose of 25 mg/kg in blood and fat, which may suggest a potential saturation at this highest dose of *trans*-permethrin. However, in brain, the normalized concentrations of *trans*-permethrin are similar at the three dosages.

Calibration of the extended PBPK models

The extended PBPK models were calibrated to the measured concentrations of *cis*- and *trans*-permethrin, and the metabolites. The values of the convergence criterion $\hat{R}$ computed for all parameters ranged between 1.0 and 1.1 indicating that the convergence was reached. The posterior distributions of the estimated parameters are reported in Table 2 and Table 3. All the posterior distributions showed coefficients of variation under 20%. As expected, the coefficients of variation were higher for parameters related to tissues such as slowly perfused tissues for which no experimental data was available. Even if less kinetic data were available for metabolites compared to

permethrin, the estimated posterior distributions of parameters related to DCCA, 3-PBA, and 4'-OH-PBA were narrowed, especially for the fraction of metabolites formed from the total clearance of permethrin. Among all parameters, the fraction of metabolites formed ($Frac_{met}$) was the sole one to be assigned to a prior uniform distribution. Following model calibration, the estimated coefficient of variation for $Frac_{met}$ for each metabolite was under 10%, indicating that the measured data on metabolites in urine were informative.

Toxicokinetic profiles of cis- *and* trans-*permethrin*

The estimated concentrations of permethrin isomers using the PBPK model were in good agreement with the observed concentrations for all the fluids and organs (Figure 2). The estimated area under the curve (AUC_{est}) was comparable to the observed AUC_{obs} and differed only by 6% in kidneys to 21% in blood for *cis*-permethrin, and by 5% in brain to 26% in fat for *trans*-permethrin (Table 5). Based on the AUC_{est}, the internal exposure of *cis*-permethrin is estimated to be higher than that for *trans*-permethrin, by a 2.8- to a 15.6-factor in blood and kidneys, respectively. For brain, fat, kidneys and liver, this factor exceeded 7. Such differences in tissue distribution trends were reflected in the model estimated values of the tissue partition coefficients. It should be noted that for *trans*-permethrin, no data were available in the liver and testes; only one time point was available in the kidneys with all other samples below the LOQ. These results were then affected by uncertainties and the AUC_{est} could even be lower for *trans*-permethrin especially in testes and liver.

Both *cis* and *trans* isomers were rapidly absorbed in the intestines, and also rapidly eliminated in liver. The estimated values for the rate of the intestinal absorption (K_{int}) for the *cis* and *trans* isomers are at 0.52 h^{-1} and 1.3 h^{-1}, respectively. The *in vivo* hepatic clearances were estimated at 5.7 L/h/kg (confidence interval at 95% [5.0; 6.4]) and 2.4 L/h/kg (confidence interval at 95% [2.2; 2.7]) for *trans*- and *cis*-permethrin respectively. The 2.4-ratio estimated between these two clearances is in the same range as that of the 2.8-ratio estimated between the *in vitro* hepatic clearances of isomers of permethrin measured using rat hepatic microsomes (Scollon *et al.*, 2009) but slightly lower compared to that observed (3.9-ratio) in rats exposed to a mixture of the two permethrin's isomers (Tornero-Velez *et al.*, 2012).

Both *cis* and *trans* isomers accumulated in fat with a partition coefficient (PC_{fat}) value of 225 and 76, respectively, and a high half-life value of 124 h and 24 h, respectively. These results are typical of the kinetics of pyrethroids in lipophilic tissues. However, our calibrated PBPK model over-estimated the concentrations in *trans*-permethrin in fat. While several assumptions were tested for the model calibration to reduce the over-estimation, no satisfactory result was achieved without diminishing the predictions accuracy in other organs and fluids. This can be a consequence of the absence of accumulation of permethrin in the muscle. The partition coefficients in muscle were around 1 and the permeability was higher compared to the values estimated for fat, brain and testes.

No parent compound was detected in urine which is consistent with previous observations of Leng *et al*. (2005). Complete excretion of *cis*- and *trans*-permethrin into feces 24 h after the administration, with a total recovery of 39% (for the dose of 4.6 mg for both isomers) after 6 days, was consistent with the estimated oral bioavaibility of 61% for permethrin as observed by Anadon *et al.* (1991).

Toxicokinetic profiles of the metabolites cis-*DCCA,* trans-*DCCA, 3-PBA and 4'-OH-PBA*

The estimated posterior distributions of the model parameters related to metabolites are summarized in Table 3. Estimated values of parameters for DCCA allowed for satisfactory model predictions of the DCCA kinetics in blood and liver (Figure 3). *Cis*- and *trans*-permethrin were mainly transformed into metabolites DCCA and 4'-OH-PBA. The estimated metabolite fraction for DCCA and 4'-OH-PBA, calculated as formed from the total clearance of each isomer of permethrin, is 0.22 and 0.29, respectively, following an exposure to *cis*-permethrin, and 0.52 and 0.45 after an exposure to *trans*-permethrin. With an estimated metabolite fraction 10 to 40 times lower, 3-PBA was produced to a lesser extent. By applying these fractional factors to the liver clearances of permethrin, the rates of formation of DCCA, 4'-OH-PBA and 3-PBA in rats were estimated at 0.53, 0.70, and 0.01 L/h/kg, respectively, after an exposure to *cis*-permethrin and at 2.96, 2.57 and 0.27 L/h/kg after an exposure to *trans*-permethrin. Due to the higher clearance of *trans*-permethrin, *trans*-DCCA was recovered in higher amount in blood and liver than *cis*-DCCA, with an AUC_{est} ratio *trans:cis* of 5 in liver and 8 in blood (Table 5). Mainly formed in the liver, *cis*- and *trans*-DCCA both accumulated in this organ and

the values of partition coefficients of *cis*-DCCA and *trans*-DCCA were estimated to be 6.3 and 4.4, respectively.

The predictions of metabolites amounts in urine are in a good agreement with the observations (Figure 4). The excretion of the metabolites was completed in the first 24 hours in urine and 48 hours in feces. For both isomers, 4'-OH-PBA was the most recovered metabolites in urine, with a 5- and a 10-factor compared respectively to *cis*-DCCA and 3-PBA in the case of *cis*-permethrin. DCCA was mainly excreted in feces. 76% of *cis*-DCCA and 62% of *trans*-DCCA of the total DCCA eliminated for each isomer was recovered in feces. In feces, 3-PBA was not detected. Gaughan *et al.* (1977) observed however that both the metabolites DCCA and 3-PBA were in a largest amount in urine compared to feces, after the oral ingestion of radiolabeled *cis* or *trans*-permethrin.

Model verification

The extended PBPK model and the estimated values of model parameters for both isomers were used to simulate the observed concentrations of permethrin isomers in blood, brain, liver and fat after the co-administration of both isomers at 1 and 10 mg/kg (*cis*/*trans* 40:60) (Tornero-Velez *et al.*, 2012). The model predictions in comparison to the observed data used for model evaluation are represented in Figure 5.

The toxicokinetic profiles predicted with the calibrated extended PBPK model (grey curves on Figure 5) were frequently not in good agreement with observed data. Specifically, the concentrations in the elimination phase of permethrin in organs were over-predicted and the ones in the absorption phase were markedly under-predicted in blood, liver and brain, between the data and model predictions. The extended model was further evaluated by adopting the absorption parameters values used in the model developed for similar pyrethroids (Mirfazaelian *et al.*, 2006), *i.e.*, the rate constant for the stomach-intestine transfer (K_{si}) and the intestinal absorption (K_{int}) were set to 0.7 h^{-1} and 0.9 h^{-1}, respectively, for both isomers (black curves on Figure 5). Our originally estimated values for these parameters were quite different according to the isomer with a lower rate of the intestinal absorption (K_{int}) of 0.5 h^{-1} for *cis*-permethrin and a higher rate of 1.3 h^{-1} for *trans*-permethrin. Using these modified values for the absorption phase allowed for obtaining comparable model predictions to the

experimental data, especially for *cis*-permethrin. The predicted toxicokinetic profiles of *trans*-permethrin in blood and liver were similar to the trend in the observed concentrations even if there was a remaining degree of over-prediction. The modifications impacted less the *cis*-permethrin toxicokinetics compared to the *trans* isomer ones. In its final calibrated form, the extended PBPK model correctly reproduced the observed concentrations in blood and 3 tissues (liver, brain and fat) measured after the co-administration of a mixture of permethrin isomers (ratio 40:60) to rats. Since no specific model was added to the extended PBPK model to account of the individual versus isomers mixture exposure scenario of exposure, these results could also suggest that no metabolic interaction in liver or in blood seemed to occur or were observable *in vivo* at the ratio of 40:60 of permethrin isomers. These results are also supported by the fact that the co-incubation of both isomers would lead to a decrease by 39% of the *in vivo* hepatic clearance of *trans*-permethrin, as observed in the *in vitro* interaction study performed by Scollon *et al.* (2009). If this modification of the clearance was applied here, the consequences will be to increase the levels of *trans*-permethrin in the organs and then the increase the over-prediction of our model.

Discussion

Population is exposed to pyrethroids, which was confirmed by a frequent recovery of the metabolites of these insecticides in the human urine during biomonitoring studies. Urinary metabolites like 3-PBA and DCCA are known to be biomarkers of exposure to pyrethroids, due to the short time of residence of the parent compound in the body. Since the toxic properties of pyrethroids are directly related to the parent compound, a proper characterization of the kinetic of permethrin in the body is required. The development of a PBPK model including both the active compound and the ones considered as biomarkers of exposure was deemed relevant. The existence of different isomeric forms of permethrin and the documented metabolic interaction between them warrants the need for assessing the kinetic of each isomer of permethrin separately. We therefore proposed to adapt a former PBPK for permethrin in rats (Tornero-Velez *et al.*, 2012) to the two major isomers of permethrin (*cis* and *trans*) separately and further extend it by including models for the corresponding urinary metabolites, 3-PBA, DCCA, and 4'-OH-PBA. The free form of metabolites of pyrethroids is commonly measured in biomonitoring studies (Heudorf *et al.*, 2006; Morgan, 2012); therefore this form was retained in this study to facilitate future uses of the developed PBPK model in a risk assessment context.

The PBPK model previously developed for deltamethrin and permethrin (Mirfazaelian *et al.*, 2006; Tornero-Velez *et al.*, 2012) was extended to describe the kinetics of the metabolites (DCCA, 3-PBA and 4'OH-PBA), and also to include additional information on tissues such as muscle, testes and kidneys in rats that were not investigated previously. Whereas the prior published PBPK models of pyrethroids were calibrated by visual fitting, the extended model was fitted to the experimental data in a Bayesian framework. This approach consists of assigning prior distributions to all parameters to be estimated and updating these distributions with the experimental data and the PBPK model through the Bayes theorem. Bayesian calibration has been successfully applied to PBPK models and has shown to be able to inform parameters related to the major ADME processes, such as metabolic rates (Brochot and Bois, 2005; Brochot *et al.*, 2007). In such complex calibration processes where data have been collected in different tissues or have been generated in different studies, an automatic

calibration approach such as the one employed here should be preferable to not overweight some data (that are subject to experimental error) and constrain the model fitting.

The calibration of the extended model was performed simultaneously using experimental data in all the measured fluids and organs and for all the chemical species relative to a specific isomer. The estimated kinetic profiles of both isomers were in good agreement with the data and consistent with observations in previous studies (Gaughan *et al.*, 1977; Anadon *et al.*, 1991; Tornero-Velez *et al.*, 2012). The kinetic profile comprised of a rapid absorption, a large accumulation in fat and a longer residence time for the *cis* isomer compared to the *trans* one. The quantification of permethrin in additional organs such as the muscle, testes and kidneys and its detection in the brain indicated that permethrin does cross the blood-testis barrier and it could pose an issue during critical time windows for developmental effects. The kidney tissue was found to behave like liver, making it a good surrogate for richly perfused tissues. Our results also underlined that permethrin does not accumulate in muscle, although it distribution was always associated with a high tissue:blood partition coefficient values, computed from experiments with 10-day-old rats exposed to deltamethrin (Mirfazaelian *et al.*, 2006; Tornero-Velez *et al.*, 2012). However muscle still remains a major compartment of the PBPK model since it comprises a large proportion (40%) of the body mass. Our model was however not able to reproduce correctly the *trans*-permethrin kinetics in fat and over-estimated the concentrations for the initial few hours after the exposure. No optimization was performed to improve the model fit in fat because the Bayesian framework ensures that the fit to the data was made simultaneously in all compartments with the same weight, without favoring a specific organ as the site of metabolism. This over-estimation can be a result of the lack of detection of *trans*-permethrin in several tissues (liver, kidneys, and testes) that can lead an under-estimation of the levels in those organs. The absence of liver concentrations above the LOQ for *trans*-permethrin also increase the uncertainty in the hepatic clearance compared to the *cis* isomer. A ratio of 2.4 was estimated for the values of the hepatic clearance of the *cis* and *trans* isomers, which is similar to the estimated ratio of 2.8 calculated from *in vitro* hepatic clearance measurements for isomers of permethrin using rat hepatic microsomes (Scollon *et al.*, 2009). The estimated values of the hepatic clearance of the isomers *cis* and *trans* are in

the same range but slightly lower than the ones obtained by extrapolating the *in vitro* clearances observed in the hepatic microsomes to *in vivo* intrinsic hepatic clearance.

The toxicokinetics of the urinary metabolites commonly used as biomarkers of exposure (DCCA and 3-PBA) were also investigated to characterize the timing of their excretion after an exposure. Both free form and newly free form after cleavage were measured without distinction in this study. Sufficient data were available to derive a simplified PBPK model for DCCA (3 compartments), and empirical models were defined for 3-PBA and 4'-OH-PBA. We chose a physiological model for DCCA in order to have available a model that could easily be extrapolated to humans and sensitive populations like children compared to empirical models. All of these models were then linked to the PBPK model of the parent compounds *via* the metabolic sites. The metabolites data were well reproduced by the models, and similar rates of formation were estimated for DCCA and 4'-OH-PBA that were significantly higher than the one for 3-PBA. Our results also pointed out that DCCA was more persistent in blood and liver than the parent compounds, and was still detected in liver 6 days after the administration for the *trans* isomer. However the urinary excretion was almost complete 2 days after the exposure. The amounts of metabolites 4'-OH-PBA, DCCA and 3-PBA as detected in urine at the end of the excretion when represented as a proportion of the sum of amounts of the three metabolites were 84%, 14% and 2%, respectively, for the *cis* isomer and 70%, 23% and 7%, respectively, for the *trans* isomer. Gaughan *et al.* (1977) had previously reported on the high recovery of 4'-OH-PBA of 43% for *trans*-permethrin and 29% for *cis*-permethrin over a large number of metabolites (compared to the 3 of our study) after administration of permethrin radiolabeled on the alcohol moiety.

Once the extended PBPK model was calibrated, the ability of our estimated set of values of parameters to reproduce the kinetic profiles of permethrin obtained in another study context was verified by using published data on isomers of permethrin in rats (Tornero-Velez *et al.*, 2012). Initial evaluation led to simulations that were not in good agreement with the published experimental concentrations partly due to differences in the absorption process. As underlined by Mirfazaelian *et al.* (2006) based on the results of a sensitivity analysis conducted on a PBPK model for deltamethrin,

blood and brain concentrations were very sensitive to the value of the stomach-intestinal constant (K_{si}) and intestinal constant (K_{int}). Since a shift in the kinetic profile was observed in the absorption phase between the two studies, the extended PBPK model was simulated using the absorption specific parameters commonly utilized for pyrethroids like deltamethrin and permethrin (Mirfazaelian *et al.*, 2006). With the estimated set of values of parameters and the absorption parameters fixed, the extended PBPK model better predicted the published concentrations (Tornero-Velez *et al.*, 2012), especially for *cis*-permethrin, the most toxic isomer (Lawrence and Casida, 1982; Soderlund *et al.*, 2002). However, the over-prediction in fat was recovered for *trans*-permethrin at the high dose of 6 mg/kg, which is consistent with the results of the calibration of the extended PBPK model. Thus, the predictive ability of the extended and calibrated PBPK model was verified for the disposition of the parent compound. The same approach was not performed for the part of the model related to the metabolites due to a lack of data for these compounds in rats in the literature. By verifying the performance of the extended model and given the similar internal exposure of permethrin isomers individually or in a mixture, a potential lack of an *in vivo* metabolic interaction between the two permethrin isomers at the ratio 40:60 was identified. However, this hypothesis needs to be evaluated by a proper interaction study in rats, at various ratios. Recently, a similar study was performed on human hepatocytes and highlighted that the interaction was negligible at the ratio 50:50 of isomers but became substantial (50% of interaction) at a ratio 10 times higher (Willemin *et al.*, 2015).

The results of our study are promising in terms of exposure assessment to permethrin and potentially to pyrethroids family. A generic structure of PBPK model for pyrethroids sharing a similar structure as permethrin seems to appear, which includes the description of the kinetic of the insecticide in fat and the sensitive organs like brain and testes. Then, the extended PBPK model developed in this study can be extrapolated to humans for the quantification of the internal exposure, especially in sensitive populations like children, by including data in humans like the recent *in vitro* results on Caco-2 cells informing on the rate of oral absorption (Zastre *et al.*, 2013), or on microsomes and hepatocytes quantifying the hepatic metabolism (Scollon *et al.*, 2009; Willemin *et al.*, 2015). With the description of the kinetic of the biomarkers of exposure under the chemical form measured in biomonitoring

studies, the extended PBPK model can be also used in a reverse dosimetry context to assess the external exposure of human populations (Ulaszewska *et al.*, 2012; Wetmore *et al.*, 2012; Wei *et al.*, 2013; Zeman *et al.*, 2013; Cote *et al.*, 2014; Huizer *et al.*, 2014). These approaches are based on the interpretation of biomonitoring data using toxicokinetic models and individual characteristics to estimate the population or individual exposure (Clewell *et al.*, 2008). Once the relevant population exposure is estimated, the extended PBPK model can be used to predict the relevant internal dosimetry of the compounds during sensitive life-stages, which will allow a better assessment of their impacts on the public health (Verner *et al.*, 2010). Performing such approach on the rat PBPK model could have confirmed the quality of predictions, but no dataset including the kinetic of both parent compound and metabolites was available in the literature at the time of this study. However, the challenge in reverse dosimetry for permethrin and pyrethroids remains to be the issue of mixtures and their potential interactions. Pyrethroids share metabolic pathways and common metabolites that can make the exposure assessment quite complicated, for example, what amount of metabolites can be attributed to a specific parent compound. Our study allowed the description of the kinetic of each isomer of permethrin separately *in vivo*, but, associated with a better understanding of the frame of the interactions between the different isomers and pyrethroids, our model could contribute to a simplification of the future exposure assessments to mixture of pyrethroids, a more realistic scenario, with PBPK models.

Aknowledgememts

This work was supported by the foundation of Université de Technologie de Compiègne “La Fondation UTC pour l’Innovation” [ToxOnChip project] and the French Ministry of Ecology and Sustainable Development [Program 190].

References

Anadon, A., Martinezlarranaga, M.R., Diaz, M.J., Bringas, P., 1991. Toxicokinetics of Permethrin in the Rat. Toxicol Appl Pharm **110**, 1-8.

Barr, D.B., Baker, S.E., Whitehead, R.D., Wong, L., Needham, L.L., 2010. Urinary Concentrations of Pyrethroid Metabolites in the General US Population, NHANES 1999-2002. Epidemiology **19**, S192-S193.

Beal, S.L., 2001. Ways to fit a PK model with some data below the quantification limit. J Pharmacokinet Pharmacodyn **28**, 481-504.

Bois, F.Y., Mazle, D.R., 1997. MCSim: A Monte Carlo Simulation Program. J Stat Softw **2**.

Bradberry, S.M., Cage, S.A., Proudfoot, A.T., Vale, J.A., 2005. Poisoning due to pyrethroids. Toxicol rev **24**, 93-106.

Brochot, C., Bois, F.Y., 2005. Use of a chemical probe to increase safety for human volunteers in toxicokinetic studies. Risk Analysis **25**, 1559-1571.

Brochot, C., Smith, T.J., Bois, F.Y., 2007. Development of a physiologically based toxicokinetic model for butadiene and four major metabolites in humans: global sensitivity analysis for experimental design issues. Chemico-biological interactions **167**, 168-183.

Brown, R.P., Delp, M.D., Lindstedt, S.L., Rhomberg, L.R., Beliles, R.P., 1997. Physiological parameter values for physiologically based pharmacokinetic models. Toxicol Ind Health **13**, 407-484.

Clewell, H.J., Tan, Y.M., Campbell, J.L., Andersen, M.E., 2008. Quantitative interpretation of human biomonitoring data. Toxicology and applied pharmacology **231**, 122-133.

Cote, J., Bonvalot, Y., Carrier, G., Lapointe, C., Fuhr, U., Tomalik-Scharte, D., Wachall, B., Bouchard, M., 2014. A novel toxicokinetic modeling of cypermethrin and permethrin and their metabolites in humans for dose reconstruction from biomarker data. PLoS One **9**, e88517.

Crow, J.A., Borazjani, A., Potter, P.M., Ross, M.K., 2007. Hydrolysis of pyrethroids by human and rat tissues: Examination of intestinal, liver and serum carboxylesterases. Toxicol Appl Pharm **221**, 1-12.

Davis, J., Tornero-Velez, R., Setzer, R.W., 2012. Computational Approaches for Developing Informative Prior Distributions for Bayesian Calibration of PBPK Models In Knaak, J.B., Timchalk, C., Tornero Velez, R., (Eds.), Parameters for Pesticide QSAR and PBPK/PD Models for Human Risk Assessment. ACS Publications, Washington, pp.

Egerer, E., Rossbach, B., Muttray, A., Schneider, M., Letzel, S., 2004. Biomonitoring of pyrethroid metabolites in environmental medicine. Umweltmed Forsh Prax **9**.

Flannigan, S.A., Tucker, S.B., Key, M.M., Ross, C.E., Fairchild, E.J., Grimes, B.A., Harrist, R.B., 1985. Synthetic Pyrethroid Insecticides - a Dermatological Evaluation. Br J Ind Med **42**, 363-372.

Gaughan, L.C., Unai, T., Casida, J.E., 1977. Permethrin Metabolism in Rats. J Agric Food Chem **25**, 9-17.

Gelman, A., Meng, X.L., Stern, H., 1996. Posterior predictive assessment of model fitness via realized discrepancies. Stat Sinica **6**, 733-760.

Godin, S.J., DeVito, M.J., Hughes, M.F., Ross, D.G., Scollon, E.J., Starr, J.M., Setzer, R.W., Conolly, R.B., Tornero-Velez, R., 2010. Physiologically Based Pharmacokinetic Modeling of Deltamethrin: Development of a Rat and Human Diffusion-Limited Model. Toxicol Sci **115**, 330-343.

Gotoh, Y., Kawakami, M., Matsumoto, N., Okada, Y., 1998. Permethrin emulsion ingestion: Clinical manifestations and clearance of isomers. J Toxicol-Clin Toxic **36**, 57-61.

He, F.S., Wang, S.G., Liu, L.H., Chen, S.Y., Zhang, Z.W., Sun, J.X., 1989. Clinical Manifestations and Diagnosis of Acute Pyrethroid Poisoning. Arch Toxicol **63**, 54-58.

Heudorf, U., Butte, W., Schulz, C., Angerer, J., 2006. Reference values for metabolites of pyrethroid and organophosphorous insecticides in urine for human biomonitoring in environmental medicine. Int J Hyg Envir Heal **209**, 293-299.

Houston, J.B., 1994. Utility of in-Vitro Drug-Metabolism Data in Predicting in-Vivo Metabolic-Clearance. Biochem Pharmacol **47**, 1469-1479.

Huizer, D., Ragas, A.M., Oldenkamp, R., van Rooij, J.G., Huijbregts, M.A., 2014. Uncertainty and variability in the exposure reconstruction of chemical incidents--the case of acrylonitrile. Toxicology letters **231**, 337-343.

Imai, K., Yoshinaga, J., Yoshikane, M., Shiraishi, H., Mieno, M.N., Yoshiike, M., Nozawa, S., Iwamoto, T., 2014. Pyrethroid insecticide exposure and semen quality of young Japanese men. Reprod Toxicol **43**, 38-44.

InVS, 2013. Exposition de la population française aux substances chimiques de l'environnement. Tome 2 : Polychlorobiphényles et Pesticides. Institut de Veille Sanitaire, pp. 178.

Jin, Y.X., Liu, J.W., Wang, L.G., Chen, R.J., Zhou, C., Yang, Y.F., Liu, W.P., Fu, Z.W., 2012. Permethrin exposure during puberty has the potential to enantioselectively induce reproductive toxicity in mice. Environ Int **42**, 144-151.

Kühn, K.H., Leng, G., Bucholski, K.A., Dunemann, L., Idel, H., 1996. Determination of pyrethroid metabolites in human urine by capillary gas chromatography-mass spectrometry. Chromatographia **43**, 285-292.

Lawrence, L.J., Casida, J.E., 1982. Pyrethroid toxicology: Mouse intracerebral structure-toxicity relationships. Pesticide Biochemistry and Physiology **18**, 9-14.

Le Grand, R., Dulaurent, S., Gaulier, J.M., Saint-Marcoux, F., Moesch, C., Lachatre, G., 2012. Simultaneous determination of five synthetic pyrethroid metabolites in urine by liquid chromatography-tandem mass spectrometry: Application to 39 persons without known exposure to pyrethroids. Toxicol Lett **210**, 248-253.

Leng, G., Gries, W., 2005. Simultaneous determination of pyrethroid and pyrethrin metabolites in human urine by gas chromatography-high resolution mass spectrometry. J Chromatogr B **814**, 285-294.

Lequesne, P.M., Maxwell, I.C., Butterworth, S.T.G., 1981. Transient Facial Sensory Symptoms Following Exposure to Synthetic Pyrethroids - a Clinical and Electro-Physiological Assessment. Neurotoxicology **2**, 1-11.

Lestremau, F., Willemin, M.-E., Chatellier, C., Desmots, S., Brochot, C., 2014. Determination of cis-permethrin, trans-permethrin and associated metabolites in rat blood and organs by gas chromatography-ion trap mass spectrometry. Anal Bioanal Chem **406**, 3477-3487.

Martignoni, M., Groothuis, G., de Kanter, R., 2006. Comparison of mouse and rat cytochrome P450-mediated metabolism in liver and intestine. Drug metabolism and disposition: the biological fate of chemicals **34**, 1047-1054.

Meeker, J.D., Barr, D.B., Hauser, R., 2008. Human semen quality and sperm DNA damage in relation to urinary metabolites of pyrethroid insecticides. Hum Reprod **23**, 1932-1940.

Mikata, K., Isobe, N., Kaneko, H., 2012. Biotransformation and enzymatic reactions of synthetic pyrethroids in mammals. Top curr chem **314**, 113-135.

Mirfazaelian, A., Kim, K.B., Anand, S.S., Kim, H.J., Tornero-Velez, R., Bruckner, J.V., Fisher, J.W., 2006. Development of a physiologically based pharmacokinetic model for deltamethrin in the adult male Sprague-Dawley rat. Toxicol Sci **93**, 432-442.

Morgan, M.K., 2012. Children's Exposures to Pyrethroid Insecticides at Home: A Review of Data Collected in Published Exposure Measurement Studies Conducted in the United States. Int J Environ Res Public Health **9**, 2964-2985.

Nakamura, Y., Sugihara, K., Sone, T., Isobe, M., Ohta, S., Kitamura, S., 2007. The in vitro metabolism of a pyrethroid insecticide, permethrin, and its hydrolysis products in rats. Toxicology **235**, 176-184.

Ross, M.K., Borazjani, A., Edwards, C.C., Potter, P.M., 2006. Hydrolytic metabolism of pyrethroids by human and other mammalian carboxylesterases. Biochem Pharmacol **71**, 657-669.

Schoeffner, D.J., Warren, D.A., Muralidara, S., Bruckner, J.V., Simmons, J.E., 1999. Organ weights and fat volume in rats as a function of strain and age. J Toxicol Environ Health A **56**, 449-462.

Scollon, E.J., Starr, J.M., Godin, S.J., DeVito, M.J., Hughes, M.F., 2009. In Vitro Metabolism of Pyrethroid Pesticides by Rat and Human Hepatic Microsomes and Cytochrome P450 Isoforms. Drug Metab Dispo **37**, 221-228.

Soderlund, D.M., 2012. Molecular mechanisms of pyrethroid insecticide neurotoxicity: recent advances. Arch Toxicol **86**, 165-181.

Soderlund, D.M., Clark, J.M., Sheets, L.P., Mullin, L.S., Piccirillo, V.J., Sargent, D., Stevens, J.T., Weiner, M.L., 2002. Mechanisms of pyrethroid neurotoxicity: implications for cumulative risk assessment. Toxicology **171**, 3-59.

Soucy, N.V., Parkinson, H.D., Sochaski, M.A., Borghoff, S.J., 2006. Kinetics of Genistein and Its Conjugated Metabolites in Pregnant Sprague-Dawley Rats Following Single and Repeated Genistein Administration. Toxicological Sciences **90**, 230-240.

Stout, D.M., II, Bradham, K.D., Egeghy, P.P., Jones, P.A., Croghan, C.W., Ashley, P.A., Pinzer, E., Friedman, W., Brinkman, M.C., Nishioka, M.G., Cox, D.C., 2009. American Healthy Homes Survey: A National Study of Residential Pesticides Measured from Floor Wipes. Environ Sci Technol **43**, 4294-4300.

Takaku, T., Mikata, K., Matsui, M., Nishioka, K., Isobe, N., Kaneko, H., 2011. In Vitro Metabolism of trans-Permethrin and Its Major Metabolites, PBalc and PBacid, in Humans. J Agric Food Chem **59**, 5001-5005.

Tornero-Velez, R., Davis, J., Scollon, E.J., Starr, J.M., Setzer, R.W., Goldsmith, M.-R., Chang, D.T., Xue, J., Zartarian, V., DeVito, M.J., Hughes, M.F., 2012. A Pharmacokinetic Model of cis- and trans-Permethrin Disposition in Rats and Humans With Aggregate Exposure Application. Toxicol Sci **130**, 33-47.

Ueyama, J., Saito, I., Kamijima, M., 2010. Analysis and evaluation of pyrethroid exposure in human population based on biological monitoring of urinary pyrethroid metabolites. J Pestic Sci **35**, 87-98.

Ulaszewska, M.M., Ciffroy, P., Tahraoui, F., Zeman, F.A., Capri, E., Brochot, C., 2012. Interpreting PCB levels in breast milk using a physiologically based pharmacokinetic model to reconstruct the dynamic exposure of Italian women. Journal of exposure science & environmental epidemiology **22**, 601-609.

US EPA, 2005. Overview of Permethrin Risk Assessment. U.S. Environmental Protection Agency, pp.

US EPA, 2011. Pesticides Industry Sales and Usage : 2006 and 2007 Market Estimates. U.S. Environmental Protection Agency, Washington, pp.

Verner, M.A., Plusquellec, P., Muckle, G., Ayotte, P., Dewailly, E., Jacobson, S.W., Jacobson, J.L., Charbonneau, M., Haddad, S., 2010. Alteration of infant attention and activity by polychlorinated biphenyls: unravelling critical windows of susceptibility using physiologically based pharmacokinetic modeling. Neurotoxicology **31**, 424-431.

Verschoyle, R.D., Aldridge, W.N., 1980. Structure-Activity-Relationships of Some Pyrethroids in Rats. Arch Toxicol **45**, 325-329.

Waites, G.M., 1991. Thermoregulation of the scrotum and testis: studies in animals and significance for man. Adv Exp Med Biol **286**, 9-17.

Wei, B., Isukapalli, S.S., Weisel, C.P., 2013. Studying permethrin exposure in flight attendants using a physiologically based pharmacokinetic model. J Expo Sci Environ Epidemiol **23**, 416-427.

Wetmore, B.A., Wambaugh, J.F., Ferguson, S.S., Sochaski, M.A., Rotroff, D.M., Freeman, K., Clewell, H.J., 3rd, Dix, D.J., Andersen, M.E., Houck, K.A., Allen, B., Judson, R.S., Singh, R., Kavlock, R.J., Richard, A.M., Thomas, R.S., 2012. Integration of dosimetry, exposure, and high-throughput screening data in chemical toxicity assessment. Toxicological sciences : an official journal of the Society of Toxicology **125**, 157-174.

Willemin, M.E., Kadar, A., de Sousa, G., Leclerc, E., Rahmani, R., Brochot, C., 2015. In vitro human metabolism of permethrin isomers alone or as a mixture and the formation of the major metabolites in cryopreserved primary hepatocytes. Toxicol In Vitro **29**, 803-812.

Wolansky, M.J., Harrill, J.A., 2008. Neurobehavioral toxicology of pyrethroid insecticides in adult animals: a critical review. Neurotoxicol Teratol **30**, 55-78.

Woollen, B.H., Marsh, J.R., Laird, W.J.D., Lesser, J.E., 1992. The Metabolism of Cypermethrin in Man - Differences in Urinary Metabolite Profiles Following Oral and Dermal Administration. Xenobiotica **22**, 983-991.

Young, H.A., Meeker, J.D., Martenies, S.E., Figueroa, Z.I., Barr, D.B., Perry, M.J., 2013. Environmental exposure to pyrethroids and sperm sex chromosome disomy: a cross-sectional study. Environ Health **12**.

Zastre, J., Dowd, C., Bruckner, J., Popovici, A., 2013. Lack of P-glycoprotein-mediated efflux and the potential involvement of an influx transport process contributing to the intestinal uptake of deltamethrin, cis-permethrin, and trans-permethrin. Toxicol Sci **136**, 284-293.

Zeman, F.A., Boudet, C., Tack, K., Floch Barneaud, A., Brochot, C., Pery, A.R., Oleko, A., Vandentorren, S., 2013. Exposure assessment of phthalates in French pregnant women: results of the ELFE pilot study. International journal of hygiene and environmental health **216**, 271-279.

Zhang, S.-Y., Ueyama, J., Ito, Y., Yanagiba, Y., Okamura, A., Kamijima, M., Nakajima, T., 2008. Permethrin may induce adult male mouse reproductive toxicity due to cis isomer not trans isomer. Toxicology **248**, 136-141.

Zhang, S.Y., Ito, Y., Yamanoshita, O., Yanagiba, Y., Kobayashi, M., Taya, K., Li, C., Okamura, A., Miyata, M., Ueyama, J., Lee, C.H., Kamijima, M., Nakajima, T., 2007. Permethrin may disrupt testosterone biosynthesis via mitochondrial membrane damage of leydig cells in adult male mouse. Endocrinology **148**, 3941-3949.

List of Figures

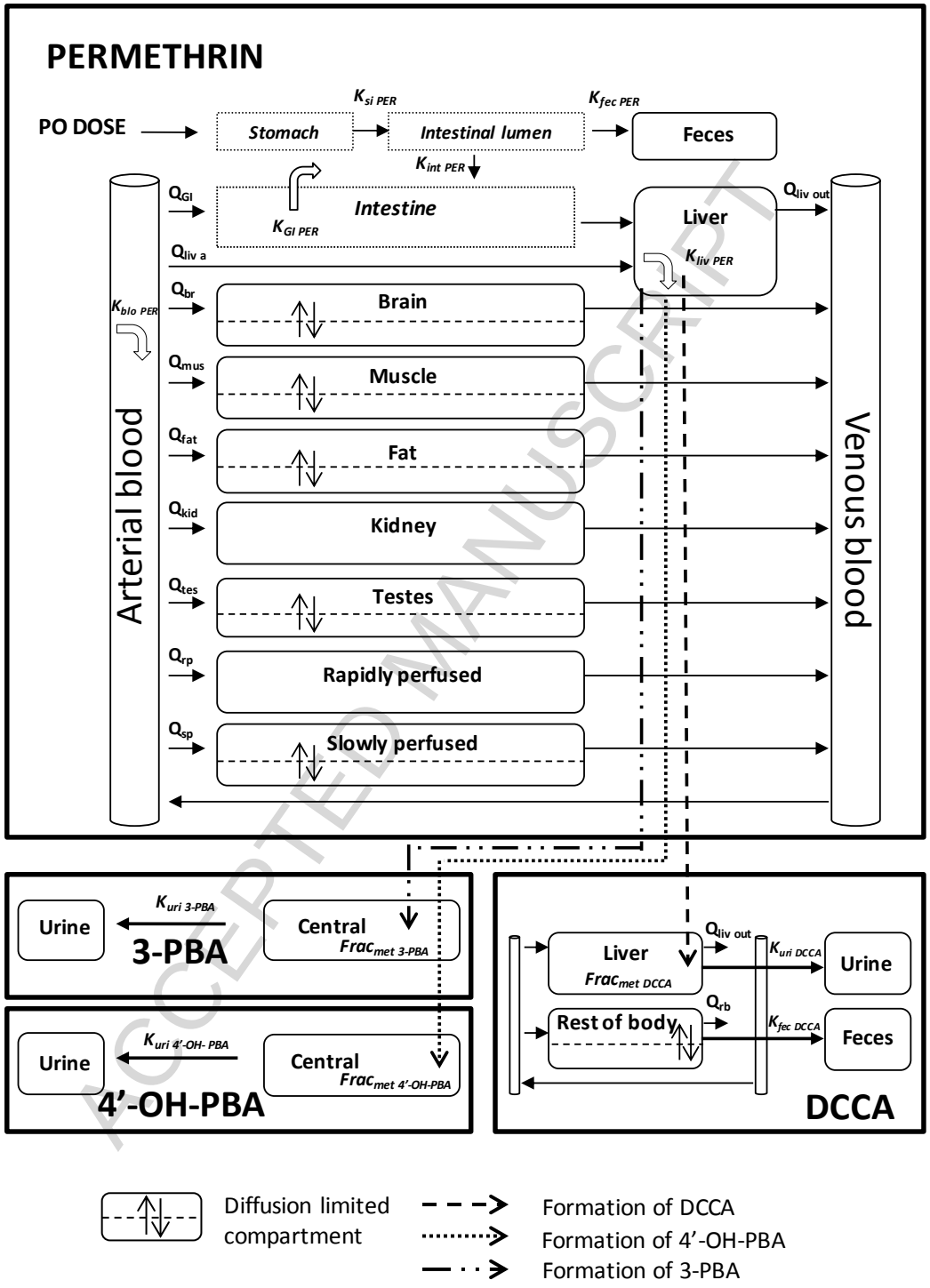

Figure 1. PBPK model of *cis*- and *trans*-permethrin (PER) and their metabolites *cis*- and *trans*-DCCA, 3-PBA and 4'-OH-PBA with an oral exposure. Distribution in brain, muscle, fat, testes and slowly perfused tissues of parent compounds and in rest of body of DCCA are limited by the diffusion and distribution in other organs by the flow. 3-PBA, DCCA, 4'-OH-PBA are formed in liver.

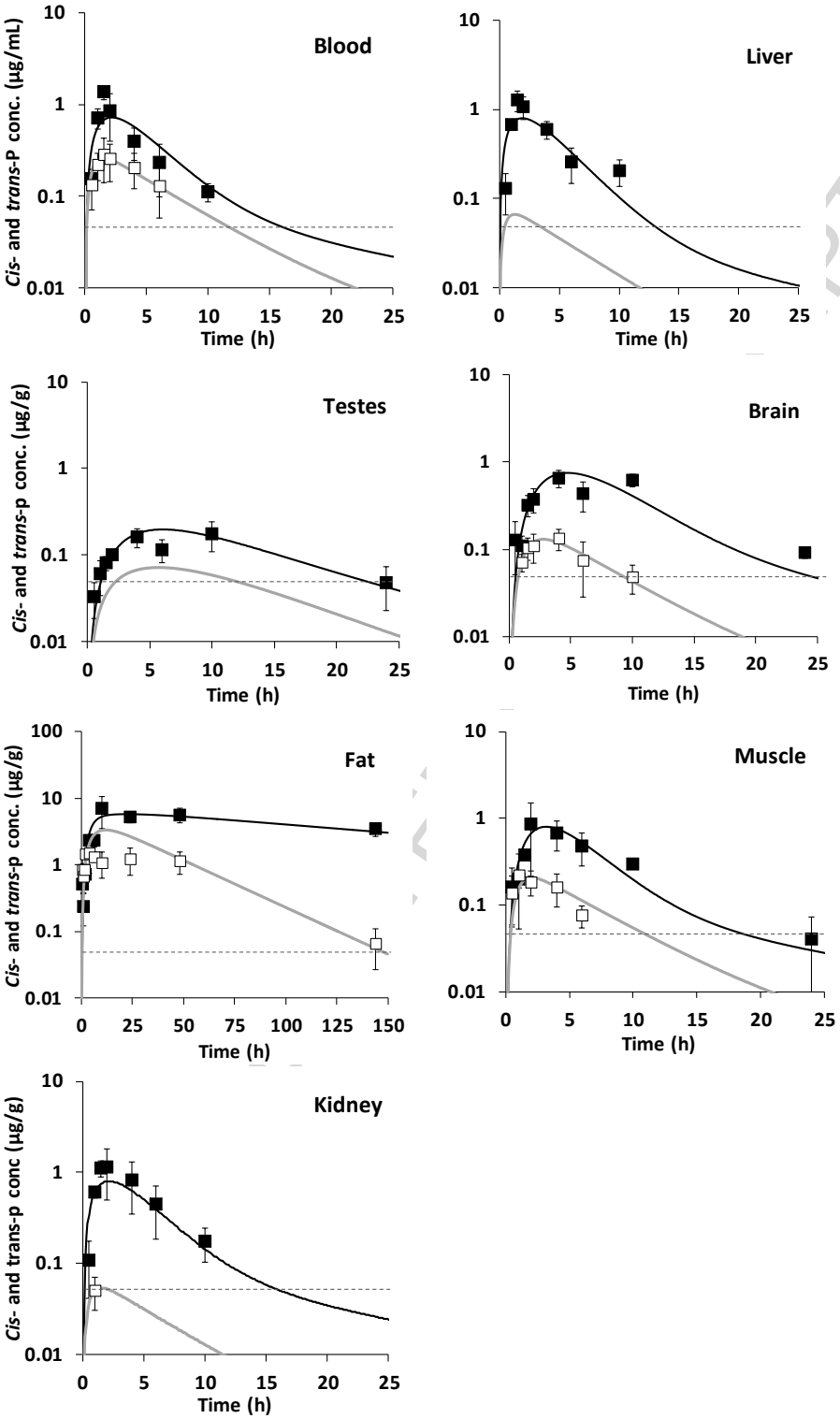

Figure 2. Measured concentrations (symbols) of *cis*-permethrin (*cis*-p) (■) and *trans*-permethrin (*trans*-p) (□) and toxicokinetic profiles estimated with the PBPK model (solid lines) of *cis*-permethrin (▬) and *trans*-permethrin (▬) in blood, liver, kidney, brain, testes, muscle and fat in rats after an exposure to 25 mg/kg of *cis* or *trans*-permethrin. The grey dotted line (- - - -) stands for the LOQ of permethrin.

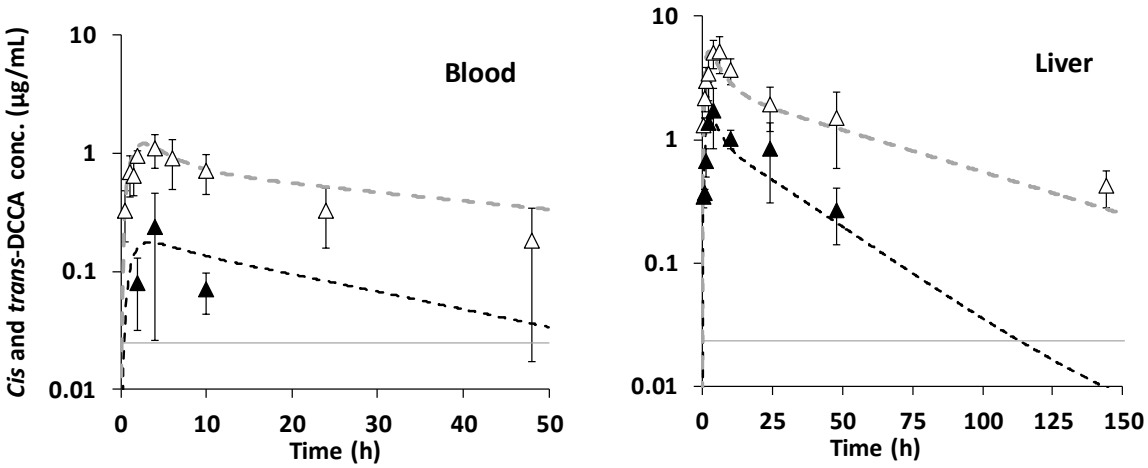

Figure 3. Measured concentrations of *cis*-DCCA (▲) and *trans*-DCCA (Δ) and toxicokinetic profiles estimated with the PBPK model of *cis*-DCCA (▬ ▬) and *trans*-DCCA (▬ ▬) in blood and liver in rats after an exposure to 25 mg/kg of *cis* or *trans*-permethrin. The grey solid line (▬) stands for the LOQ of DCCA.

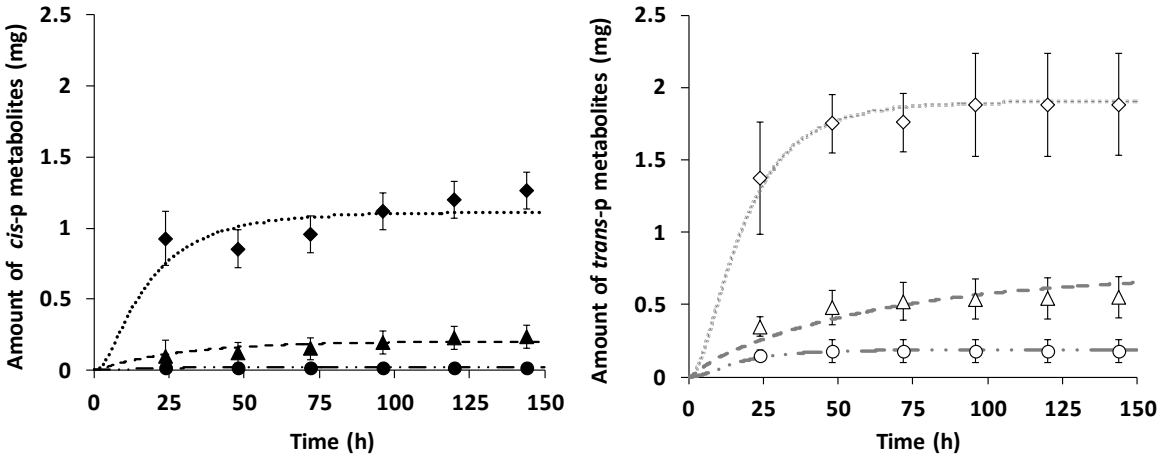

Figure 4. Kinetics of observed amounts in the metabolites 4'-OH-PBA (◊), DCCA (Δ) and 3-PBA (○) and estimated amounts in 4'-OH-PBA (..), DCCA (▬ ▬) and 3-PBA (▬ . . ▬) in urine in rats after an exposure to 25 mg/kg of *cis* or *trans*-permethrin. Closed symbols and black lines are related to *cis*-permethrin (*cis*-p) and open symbols and grey lines to *trans*-permethrin (*trans*-p).

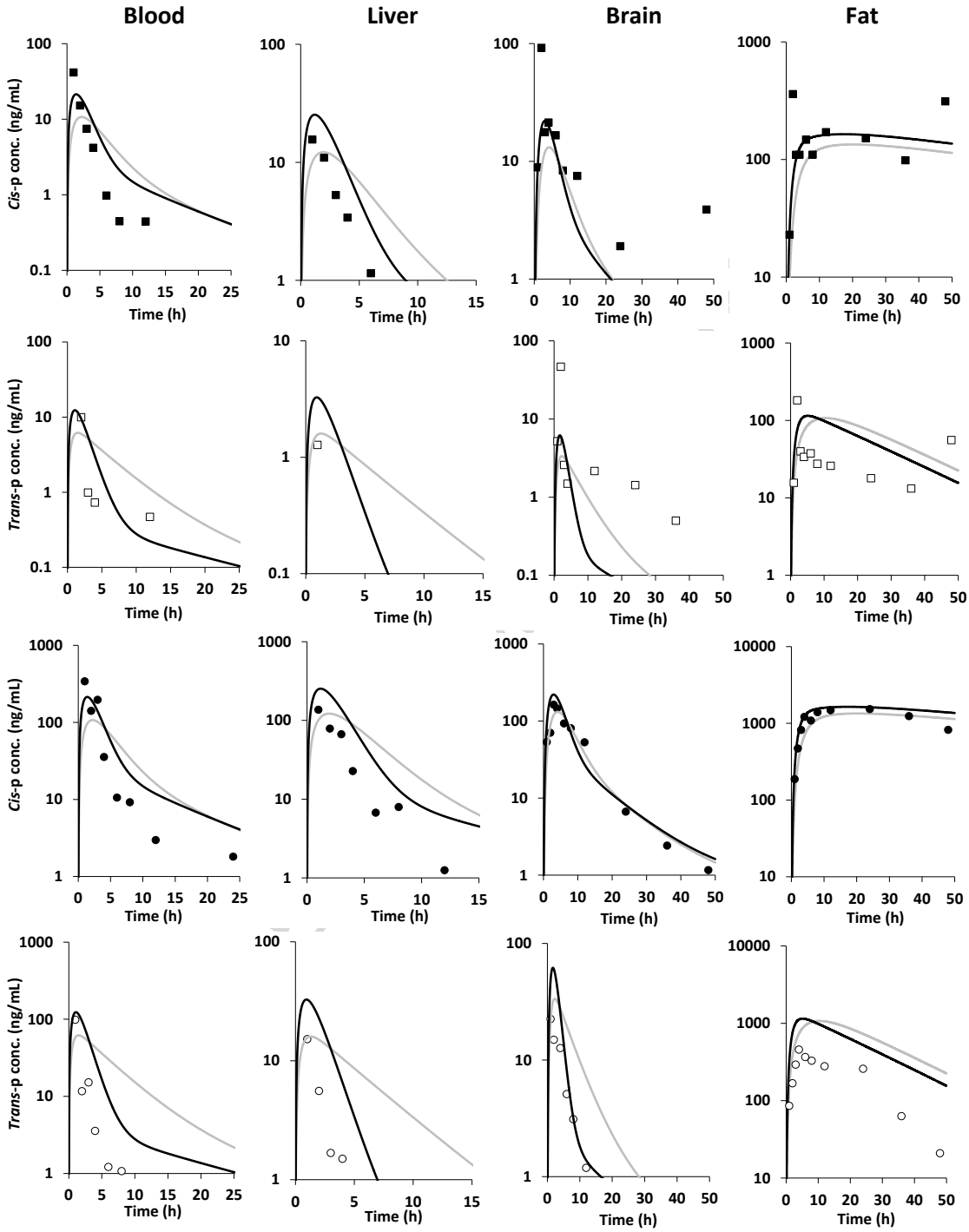

Figure 5. Observed concentrations in blood, liver, brain and fat after an oral dose of *cis*-permethrin at 0.4 mg/kg (■) and 4 mg/kg (●) and of *trans*-permethrin at 0.6 mg/kg (□) and 6 mg/kg (○).The observed data are issued from the study of Tornero-Velez *et al.* (2012). The predicted concentrations from the values of parameters estimated with the extended PBPK model of permethrin and metabolites (▬) and with the extended PBPK model with absorption rate fixed (▬) are also represented.

List of Tables

Table 1. Physiological parameters for PBPK models of *cis*- and *trans*-permethrin and metabolites *cis*- and *trans*-DCCA, 3-PBA and 4'-OH-PBA in rats.

Parameters	**Value**	**Source**
Body Weight (BW) (kg)	0.47	Exp data
Total cardiac flow (Q_c, L/h/kg$^{0.75}$)	14.1	Brown *et al.* (1997)
Relative tissue volumes (% of BW)		
Blood (V_{blo})	7.4	Brown *et al.* (1997)
Brain (V_{bra})	0.4	Exp data
Fat (V_{fat})	7.0	Brown *et al.* (1997)
Kidney (V_{kid})	0.6	Exp data
GI tract (V_{gi})	2.7	Brown *et al.* (1997)
Liver (V_{liv})	3.5	Exp data
Muscle (V_{mus})	40.4	Brown *et al. (1997)*
Testes (V_{tes})	0.8	Exp data
Non perfused	5	Brown *et al.* (1997)
Rapidly perfused (V_{rp})	4.6	Brown *et al.* (1997)
Slowly perfused (V_{sp})	27.6	1 - all organs - non perfused
Rest of body [a] (V_{rb})	89.1	1 - blood - liver - non perfused
Tissue blood flow (% cardiac output)		
Brain (Q_{bra})	2.0	Brown *et al.* (1997)
Fat (Q_{fat})	7.0	Brown *et al.* (1997)
Kidney (Q_{kid})	14.1	Brown *et al.* (1997)
Liver (total) ($Q_{liv\ out}$)	17.5	Brown *et al.* (1997)
Portal (GI tract) (Q_{gi})	15.1	
Arterial ($Q_{liv\ a}$)	2.4	
Muscle (Q_{mus})	27.8	Brown *et al.* (1997)
Testes (Q_{tes})	0.4	Waites (1991)
Rapidly perfused (Q_{rp})	24.9	1 - all organ flows
Slowly perfused (Q_{sp})	6.3	Brown *et al. (1997)*
Rest of body [a] (Q_{rb})	82.6	1 - total liver flow
Blood volume fraction (% of tissue)		
Brain (BV_{bra})	3	Brown *et al.* (1997)
Fat (BV_{fat})	2	Tornero-Velez *et al.* (2012)
Slowly perfused (BV_{sp})	4	Assimilated to muscle Tornero-Velez *et al.* (2012)
Testes (BV_{tes})	4	Assimilated to muscle Tornero-Velez *et al.* (2012)
Rest of body [a] (BV_{rb})	5	

[a]: only for the PBPK model of the metabolite DCCA.

Note: GI tract tissue volume contains stomach, small and large intestines. Volume of the rapidly perfused tissues stands for heart, lung, adrenal, trabecular bone, marrow, pancreas, spleen and thyroid. Volume of the non perfused tissues stands for the GI tract content. Flow of slowly perfused tissues stands for cortical bones and skin. Rest of body corresponds to all the organs except liver.

Table 2. Distributions of the *cis*- and *trans*-permethrin specific parameters of the PBPK model in rats. All prior distributions of parameters are truncated normal distributions represented by the average value ± SD and their boundaries. Posterior distributions are represented by the mean with the 2.5th and 97.5th percentiles.

Parameters	***Prior distribution***		***Posterior distribution***	
	Cis-Permethrin	*Trans*-Permethrin	*Cis*-Permethrin	*Trans*-Permethrin
Partition coefficients				
Brain:blood (PC_{bra})	0.4 ± 0.2 [10^{-3} - 30]	0.4 ± 0.2 [10^{-3} - 30]	**1.6** [1.4 - 1.8]	**0.57** [0.49 - 0.66]
Fat:blood (PC_{fat})	150 ± 75 [5 - 500]	50 ± 25 [5 - 500]	**225** [171 – 301]	**76** [69 - 85]
GI:blood (PC_{gi})	Equal to PC_{kid}	Equal to PC_{kid}	-	-
Kidney:blood (PC_{kid})	0.4 ± 0.2 [10^{-3} - 30]	0.4 ± 0.2 [10^{-3} - 30]	**1.1** [1.0 - 1.2]	**0.21** [0.16 - 0.27]
Liver:blood (PC_{liv})	0.4 ± 0.2 [10^{-3} - 30]	Equal to PC_{kid}	**0.89** [0.80 - 0.99]	-
Muscle:blood (PC_{mus})	6 ± 3 [10^{-3} - 30]	6 ± 3 [10^{-3} - 30]	**1.2** [1.0 - 1.5]	**0.82** [0.70 - 0.95]
Testes:blood (PC_{tes})	0.4 ± 0.2 [10^{-3} - 30]	Equal to PC_{bra}	**0.63** [0.54 - 0.72]	-
Rapidly perfused:blood (PC_{rp})	Equal to PC_{kid}	Equal to PC_{kid}	-	-
Slowly perfused:blood (PC_{sp})	6 ± 3 [10^{-3} - 30]	6 ± 3 [10^{-3} - 30]	**19** [15 - 23]	**8.4** [2.4 - 14.2]
Permeability coefficients (L/h)				
Brain (PA_{bra})	10^{-3} ± 10^{-3} [10^{-5} - 1]	10^{-3} ± 10^{-3} [10^{-5} - 1]	**$1.0.10^{-3}$** [$8.4.10^{-4}$ - $1.3.10^{-3}$]	**$1.2.10^{-3}$** [$0.8.10^{-3}$ - $1.6.10^{-3}$]
Fat (PA_{fat})	0.1 ± 0.1 [10^{-5} - 1]	0.1 ± 0.1 [10^{-5} - 1]	**$4.8.10^{-2}$** [$4.3.10^{-2}$ - $5.4.10^{-2}$]	**0.11** [0.09 - 0.12]
Muscles (PA_{mus})	0.1 ± 0.1 [10^{-5} - 1]	0.1 ± 0.1 [10^{-5} - 1]	**0.32** [0.21 - 0.47]	**0.48** [0.38 - 0.60]
Testes (PA_{tes})	10^{-3} ± 10^{-3} [10^{-5} - 1]	Equal to PA_{bra}/3	**$3.3.10^{-4}$** [$2.7.10^{-4}$ - $4.0.10^{-4}$]	-
Slowly perfused (PA_{sp})	0.1 ± 0.1 [10^{-5} - 1]	0.1 ± 0.1 [10^{-5} - 1]	**0.31** [0.22 - 0.41]	**0.065** [9.10^{-3} - 0.19]
Rate constants (h^{-1})				
Stomach-intestine transfer (K_{si})	0.5 ± 0.25 [0 - 2]	0.5 ± 0.25 [0 - 2]	**0.35** [0.30 - 0.40]	**0.20** [0.17 - 0.23]
Intestinal absorption (K_{int})	0.5 ± 0.25 [0 - 2]	0.5 ± 0.25 [0 - 2]	**0.52** [0.43 - 0.63]	**1.30** [1.1 - 1.6]
Fecal excretion (K_{fec})	0.5 ± 0.25 [0 - 2]	0.5 ± 0.25 [0 - 2]	**0.39** [0.31 - 0.47]	**0.85** [0.68 - 1.06]
Metabolic clearances				
GI metabolism (L/h/kg) (K_{gi})	Fixed to 0.04	Fixed to 0.3	-	-
Blood metabolism (L/h/kg) (K_{blo})	Fixed to 0.07	Fixed to 0.29	-	-
Liver metabolism (L/h/kg) (K_{liv})	3 ± 3 [10^{-5} - 20]	10 ± 10 [10^{-5} - 40]	**2.4** [2.2 - 2.7]	**5.7** [5.0 - 6.4]

Table 3. Distributions of the specific parameters of DCCA, 3-PBA and 4'-OH-PBA of the PBPK model in rats. The prior distributions of all parameters are truncated normal distributions represented by the average value ± SD and their boundaries, except the rate of formation of metabolites represented by a uniform distribution. Posterior distributions are represented by the mean with the 2.5th and 97.5th percentiles.

Parameters	***Prior distribution***			***Posterior distribution***		
	DCCA	**3-PBA**	**4'-OH-PBA**	**DCCA**	**3-PBA**	**4'-OH-PBA**
***Trans*-permethrin**						
Partition coefficients						
Liver:blood (PC_{liv})	10 ± 5 [1 - 30]	-	-	**4.4** [3.9 - 5.0]	-	-
Rest of body:blood (PC_{rb})	10 ± 5 [1 - 30]	-	-	**2.7** [2.2 - 3.3]	-	-
Permeability coefficients (L/h)						
Rest of body:blood (PA_{rb})	0.1 ± 0.1 [10^{-5} - 2]	-	-	**0.25** [0.18 - 0.34]	-	-
Fraction of metabolite formed						
Fraction ($Frac_{met}$)	[10^{-5} - 1]	[10^{-5} - 1]	[10^{-5} - 1]	**0.52** [0.46 - 0.58]	**0.048** [0.042 - 0.056]	**0.45** [0.39 - 0.53]
Rate constants						
Fecal excretion (h^{-1}) (K_{fec})	0.5 ± 0.25 [0 - 2]	-	-	**0.42** [0.36 - 0.48]	-	-
Urine excretion [a] (K_{uri})	0.05 ± 0.025 [0 - 0.2]	0.05 ± 0.025 [0 - 0.2]	0.05 ± 0.025 [0 - 0.2]	**0.017** [0.015 - 0.020]	**0.078** [0.051 - 0.114]	**0.071** [0.045 - 0.104]
***Cis*-permethrin**						
Partition coefficients						
Liver:blood (PC_{liv})	10 ± 5 [1 - 30]	-	-	**6.3** [5.3 - 7.6]	-	-
Rest of body:blood (PC_{rb})	10 ± 5 [1 - 30]	-	-	**3.4** [2.7 - 4.1]	-	-
Permeability coefficients (L/h)						
Rest of body:blood (PA_{rb})	0.1 ± 0.1 [10^{-5} - 2]	-	-	**0.85** [0.72 - 0.98]	-	-
Fraction of metabolite formed						
Fraction ($Frac_{met}$)	[10^{-5} - 1]	[10^{-5} - 1]	[10^{-5} - 1]	**0.22** [0.19 - 0.25]	**$5.4.10^{-3}$** [$4.6.10^{-3}$ - $6.3.10^{-3}$]	**0.29** [0.25 - 0.33]
Rate constants						
Fecal excretion (h^{-1}) (K_{fec})	0.5 ± 0.25 [0 - 2]	-	-	**1.0** [0.9 - 1.2]	-	-
Urine excretion [a] (K_{uri})	0.05 ± 0.025 [0 - 0.2]	0.05 ± 0.025 [0 - 0.2]	0.05 ± 0.025 [0 - 0.2]	**0.038** [0.031 - 0.047]	**0.075** [0.048 - 0.111]	**0.070** [0.044 - 0.103]

[a]: the urine clearance of the DCCA is expressed in L/h and the rate of urine elimination of 3-PBA and 4'-OH-PBA in h^{-1}.

Table 4. Half-lives ($T_{1/2}$, unit: h) of *cis*- and *trans*-permethrin and metabolites *cis*- and *trans*-DCCA in blood, brain, fat, kidney, liver, muscle and testes determined on observed concentrations. α and β are respectively assigned to the first and the second slope of the curve.

	***Cis*-Permethrin**			***Trans*-Permethrin**	***Cis*-DCCA**		***Trans*-DCCA**	
	$T_{1/2}$	$T_{1/2}\alpha$	$T_{1/2}\beta$	$T_{1/2}$	$T_{1/2}\alpha$	$T_{1/2}\beta$	$T_{1/2}\alpha$	$T_{1/2}\beta$
Blood	-	1.5	3.3	4.2	3.4	-	12.0	30.1
Brain	7.2	-	-	4.3	-	-	-	-
Fat	139	-	-	23.1	-	-	-	-
Kidney	2.9	-	-	- [a]	-	-	-	-
Liver	-	2.0	11.7	- [a]	17.8	-	13.6	53.3
Muscle	5.0	-	-	3.5	-	-	-	-
Testes	12.0	-	-	- [a]	-	-	-	-

[a]: no half-life was computed because no compound was detected

Table 5. Average and standard deviation of values of the pharmacokinetic parameters the area under the curve of the observed concentrations (AUC_{obs}) and the estimated concentrations (AUC_{est}) (µg.h/mL) of *cis*- and *trans*-permethrin and *cis*- and *trans*-DCCA vs times in blood, brain, fat, kidney, liver, muscle and testes.

	***Cis*-permethrin**		***Trans*-permethrin**		***Cis*-DCCA**		***Trans*-DCCA**	
	AUC_{obs}	**AUC_{est}**	**AUC_{obs}**	**AUC_{est}**	**AUC_{obs}**	**AUC_{est}**	**AUC_{obs}**	**AUC_{est}**
Blood	4.5	5.5 ± 0.1	1.8 [a]	2.0 ± 0.1	1.7	5.4 ± 0.6	37.5	41.4 ± 2.7
Brain	10.2	8.7 ± 0.5	1.1 [a]	1.2 ± 0.08	-	-	-	-
Fat	1366 [a]	1180 ± 162	117	148 ± 7	-	-	-	-
Kidney	6.4	6.0 ± 0.3	-	0.41 ± 0.06	-	-	-	-
Liver	5.9 [a]	5.0 ± 0.2	-	0.45 ± 0.06	45.1	34.8 ± 2.1	245.8	184 ± 10
Muscle	7.5	6.6 ± 0.5	1.4 [a]	1.6 ± 0.1	-	-	-	-
Testes	3.3	3.5 ± 0.2	-	1.2 ± 0.8	-	-	-	-

[a]: value of extrapolated AUC was over 20% but not exceeded 50% of the total AUC.

Note: AUC_{obs} was defined as the sum of the AUC computed with the trapezoidal rule on observed concentrations and the AUC_{est}, defined as the last observed concentration divided by the elimination rate.

Highlights

- A PBPK model of isomers of permethrin and its urinary metabolites was developed
- A quantitative link was established for permethrin and its biomarkers of exposure
- The bayesian framework allows getting confidence interval on the estimated parameters
- The PBPK model can be extrapolated to human and used in a reverse dosimetry context